

SSFMamba: Symmetry-driven Spatial-Frequency Feature Fusion for 3D Medical Image Segmentation

Bo Zhang¹, Yifan Zhang¹, Shuo Yan¹, Yu Bai¹, Zheng Zhang², Wu Liu³, Xiuzhuang Zhou²,
Wendong Wang¹

¹ State Key Laboratory of Networking and Switching Technology, School of Computer Science (National Pilot Software Engineering School), Beijing University of Posts and Telecommunications.

² School of Intelligent Engineering and Automation, Beijing University of Posts and Telecommunications.

³ School of Information Science and Technology, University of Science and Technology of China.
zbo@bupt.edu.cn, zylf4n@bupt.edu.cn, shuoyan@bupt.edu.cn, by@bupt.edu.cn, zhangzheng@bupt.edu.cn, liuwu@ustc.edu.cn, xiuzhuang.zhou@bupt.edu.cn, wdwang@bupt.edu.cn

Abstract

In light of the spatial domain’s limited capacity for modeling global context in 3D medical image segmentation, emerging approaches have begun to incorporate frequency domain representations. However, straightforward feature extraction strategies often overlook the unique properties of frequency domain information, such as conjugate symmetry. They also fail to account for the fundamental differences in data distribution between the spatial and frequency domains, which can ultimately dilute or obscure the complementary strengths that frequency-based representations offer. In this paper, we propose SSFMamba, a **Mamba** based **S**ymmetry-driven **S**patial-Frequency feature fusion network for 3D medical image segmentation. SSFMamba employs a complementary dual-branch architecture to extract features from both the spatial and frequency domains, and leverages a Mamba block to fuse these heterogeneous features to preserve global context while reinforcing local details. In the frequency domain branch, we harness Mamba’s exceptional capability to extract global contextual information in conjunction with the synergistic effect of frequency domain features to further enhance global modeling. Moreover, we design a 3D multi-directional scanning mechanism to strengthen the fusion of local and global cues. Experiments on the BraTS2020 and BraTS2023 datasets demonstrate that SSFMamba consistently outperforms state-of-the-art methods across various metrics.

1 Introduction

The aim of 3D medical image segmentation is to accurately delineate the complex anatomical structures of organ or tumor, which requires not only fine-grained modeling of local details but also a holistic understanding of spatial relationships. Recent studies that rely solely on spatial domain information are effective at capturing local features, but they often fall short in modeling long-range dependencies—particularly in high-resolution, large-volume 3D medical images, leading to challenges such as inaccurate boundary delineation, difficulty in handling complex or spatially extended structures, and a tendency to overfit to local patterns. For example, CNN models (LeCun, Bengio et al. 1995) can effectively capture local features, but are inherently limited when modeling long-range dependencies. In contrast, Transformer models (Vaswani et al. 2017)

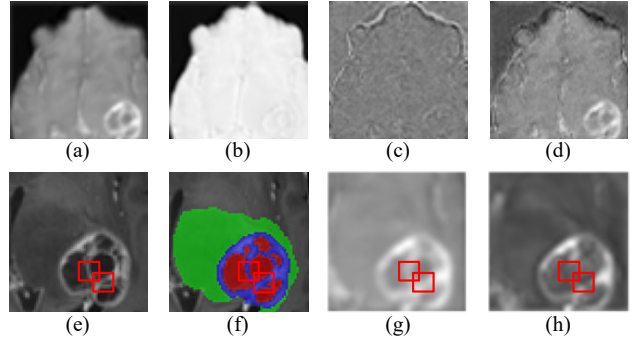


Figure 1: Feature maps of: (a) origin image, (b) spatial domain, (c) frequency domain, (d) fused multi-domain; and (e) origin image; (f) annotation; (g) our feature map; (h) SegMamba’s feature map. Spatial domain can provide comprehensive representation but exhibit blurred boundaries; frequency domain can provide clear boundaries and high-contrast details, and the fused features can effectively emphasize the tumor region and its peripheral contours by integrating both representations.

are highly effective at modeling global context but suffer from quadratic computational complexity, which becomes prohibitively expensive when applied to 3D medical images with large voxel counts—especially, especially when there are more complex situations such as multimodality. Recently, Mamba models (Gu and Dao 2024) have demonstrated strong capabilities in modeling long-range dependencies by leveraging a state-space formulation combined with a selective computation mechanism. However, Mamba is sensitive to the ordering of input sequences, and the conversion of spatial structures into one-dimensional sequences presents challenges for preserving and effectively modeling spatial relationships.

To overcome the restricted receptive field and lack of global awareness in spatial domain models, frequency domain analysis has garnered increasing attention. Compared to natural images, the utility of frequency domain features is even more pronounced in medical imaging. For instance, Magnetic resonance imaging (MRI) data are inherently acquired in the frequency domain (k-space) (Plewes

and Kucharczyk 2012), aligning frequency-based representations more closely with the physical foundation of medical images. The frequency domain facilitates effective extraction of global structures and fine details, enhancing image processing performance. For example, incorporating frequency domain information has proven effective in enhancing a model’s global perceptual capability in certain image fusion applications (Zhao et al. 2023; Zou et al. 2024a). As illustrated in Fig.1, the locally enlarged details in (e–h) demonstrate that our method preserves edge details more effectively compared to feature maps that rely solely on spatial domain information.

However, Researchers often use naive transformations such as 1×1 convolution to extract frequency domain features (Zou et al. 2024b; Chang et al. 2024), but this approach fails to fully leverage the unique characteristics of frequency data. Compared to the spatial domain, the frequency domain exhibits distinctive properties such as conjugate symmetry, compact energy concentration, and global receptive field representation. For example, while conjugate symmetry has been extensively utilized in traditional compression algorithms (Rhee et al. 2022; Velisavljevic, Beferull-Lozano, and Vetterli 2007; Xu et al. 2020), its utility in high-fidelity image processing remains largely untapped, representing a missed opportunity for further performance improvements.

These properties offer the potential for more efficient encoding of structural and contextual information. Meanwhile, the frequency domain also introduces nontrivial challenges: its semantic representations are less intuitive, and its data distributions fundamentally differ from those in the spatial domain. Consequently, naive integration with spatial features may dilute or obscure the complementary strengths of frequency-based representations.

To address the aforementioned challenges, we propose Symmetry-driven Spatial-Frequency Feature Fusion Mamba (SSFMamba), as illustrated in Fig.2. SSFMamba employs the Mamba module to extract features from frequency domain representations and fully harness its global context extraction capabilities and the synergistic advantages of frequency domain structural information to enhance global feature modeling. Therefore, we have optimized the architectural design so that Mamba can efficiently process and integrate information from both spatial and frequency domains, achieving deep coupling and synergistic enhancement of both global context and local details. Meanwhile, we observe that Mamba is highly sensitive to the order of its input sequences. By leveraging the conjugate symmetry of frequency domain data for sequence modeling, we significantly enhance its global modeling capability. Based on this property, we have designed a novel 3D multi-directional scanning mechanism that not only models the intrinsic spatial structure of 3D images in the frequency domain but also more effectively captures both global contextual information and local details. This can further increase the accuracy and robustness of our approach in 3D medical image segmentation tasks. Our main contributions are as follows:

- We propose a Mamba based dual-branch symmetry-driven spatial-frequency feature fusion network for accurate 3D medical image segmentation, which can align

and fuse both local contextual details from the spatial branch and global semantic patterns from frequency branch.

- We introduce an efficient frequency-domain feature extraction strategy to transform multi-scale 3D images via FFT, exploit the inherent conjugate symmetry of the frequency representation, then employ Mamba to extract global features, enhancing the model’s global perception and computational efficiency.
- We further design a 3D multi-directional scanning mechanism that deeply integrates frequency domain information to strengthen the fusion of local and global cues, which enhances Mamba’s local feature modeling while complementing its robust global context extraction.

2 Related Work

3D Medical Image Segmentation. Many studies focus on striking a better balance between global modeling and detail recovery, thereby providing more accurate segmentation results for practical clinical applications. In early research, CNN-based methods primarily focused on extracting local features, which significantly improved segmentation performance within the U-Net (Ronneberger, Fischer, and Brox 2015) architecture. However, these approaches are limited by the receptive fields of CNNs, making it challenging to effectively model global information. With the successful application of Transformers in computer vision, an increasing number of studies have begun exploring hybrid architectures that combine Transformers with CNNs, such as TransUNet (Chen et al. 2024). By leveraging the excellent global modeling capabilities of Transformers alongside the local modeling strengths of CNNs, segmentation performance has been further improved. However, one significant drawback of Transformers is their exponentially increasing computational complexity, which makes scaling to 3D images with a large number of pixels challenging.

In recent years, the emergence of Mamba has brought new opportunities, as it proves to be more efficient than traditional Transformer networks when dealing with large-scale 3D images (Liu et al. 2024a,b). However, its potential in 3D vision tasks remains far from fully explored.

Multi-domain Information Fusion. Traditional image processing models predominantly rely on spatial domain features due to the intuitive nature of pixel values and their well-defined spatial relationships, which have led to significant achievements across various vision tasks (Liu et al. 2021; Wenxuan et al. 2021). However, frequency domain information provides unique advantages in capturing global patterns by encoding frequency properties that are often challenging to extract using spatial domain methods alone. Frequency-based representations enhance global structure perception, thereby improving model performance and robustness.

The Fourier transform is a fundamental tool for mapping spatial data into the frequency domain, enabling the extraction of global statistical features widely utilized in denoising, segmentation, and super-resolution (Huang et al. 2022; Pratt et al. 2017; Zhou et al. 2022; Liu et al. 2023; Zou et al.

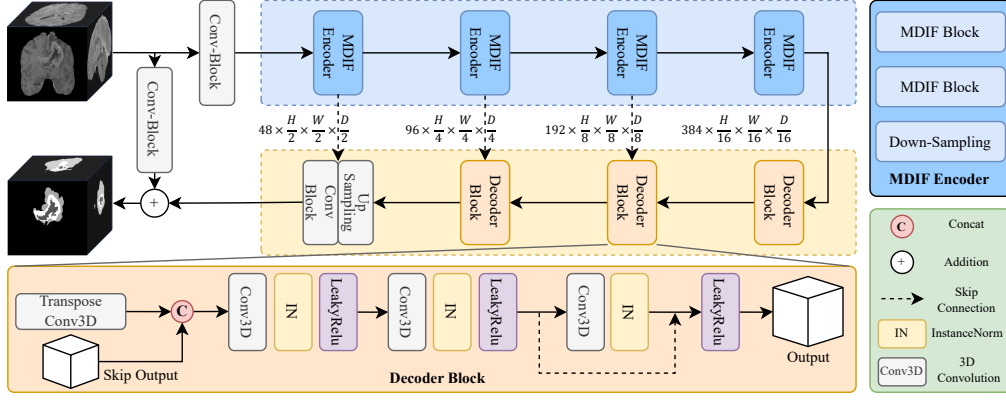


Figure 2: The overall architecture of the proposed SSFMamba.

2024b). To harness the complementary strengths of spatial precision and frequency-domain globality, many approaches fuse both domains, striking a balance between local detail preservation and global context modeling. For example, to address texture blur and color distortion in low-light conditions, dual-branch networks such as SFFNet (Yang, Yuan, and Li 2024) integrate spatial and frequency features for enhanced visual restoration. Despite notable progress in incorporating frequency domain information (Wang et al. 2023), its full potential remains underutilized. Meanwhile, the spatial domain branch focuses on local contextual relationships and fine-grained details, while the frequency domain branch emphasizes global structures and pattern properties. The integration of these two types of information creates a complementary effect, preserving intricate local details (such as edges and textures) while enhancing global perception (such as regional contrast and object contours).

State Space Models. Recent advances in Structured State Space Models (SSMs) (Gu, Goel, and Ré 2022) have garnered significant attention from both academia and industry due to their computational efficiency in long-sequence processing. Unlike traditional Transformer architectures with quadratic computational complexity $\mathcal{O}(L^2)$, SSMs achieve linear complexity $\mathcal{O}(L)$ through hidden state recursion mechanisms, reducing resource consumption in long-context scenarios. The seminal work S4 (Structured State Space Sequence Model) (Smith, Warrington, and Linderman 2023) established the foundation for modern deep learning in long-sequence modeling.

Notably, Mamba (Gu and Dao 2024), an evolved version of S4, has overcome the expressiveness limitations inherent in conventional SSMs. Empirical studies demonstrate that Mamba not only matches or surpasses Transformer performance in tasks such as language modeling and genomic analysis, but also rigorously maintains linear scalability with sequence length, offering a novel technical pathway for low-resource long-sequence inference. Mamba has transcended its original application in natural language processing, achieving remarkable progress in tasks such as image segmentation and fusion, as well as in other domains including medical imaging analysis and computer vision (Liu, Zhang, and Zhang 2024; Yue and Li 2024; Zhu et al. 2024).

3 Method

3.1 Preliminaries

Frequency Analysis Medical imaging typically exhibits complex anatomical structures, noise interference, and intensity variations between tissues. Frequency domain is of great significance to global feature extraction, noise suppression and enhancement, and multi-modal data fusion. By providing a global perspective for medical image interpretation via mathematical transformations (e.g., Fourier transform, wavelet transform), frequency domain compensates for the inherent limitations of conventional spatial domain methodologies. The 3D Fast Fourier Transform (3D FFT) is a computational algorithm that decomposes a three-dimensional image into a collection of multi-scale frequency components. For instance, consider a 3D image with dimensions $H \times W \times D$. The mathematical formulation of its 3D Discrete Fourier Transform (3D DFT) can be expressed as follows:

$$F(u, v, w) = \sum_{h=0}^{H-1} \sum_{w=0}^{W-1} \sum_{d=0}^{D-1} f(h, w, d) e^{-j2\pi(\frac{uh}{H} + \frac{vw}{W} + \frac{wd}{D})}, \quad (1)$$

where u, v and w denote the frequency indices along the height, width, and depth dimensions, respectively. Function f represents the original 3D signal in the spatial (or temporal) domain (Chi, Jiang, and Mu 2020). This process enables the synergistic representation of both global structural properties and local fine-grained details through their frequency-domain features. Moreover, when the original image contains real-valued data, its frequency domain representation exhibits conjugate symmetry (Walker 2017). Namely, the complex conjugate of a frequency component is equal to the value at its symmetric position in the frequency domain:

$$F(-u, -v, -w) = \overline{F(u, v, w)}. \quad (2)$$

This property improves the controllability of frequency-domain information in compression, enhancement, and denoising, while also providing structural constraints for model design. In the Mamba-based sequence model, this conjugate symmetry can enable more effective global context modeling when combined with a 3D Multi-Directional Scanning Mechanism.

State Space Models The SSM (Structured State Space Model, S4) utilized in Mamba extends traditional state space models by enhancing expressive power through discretizing

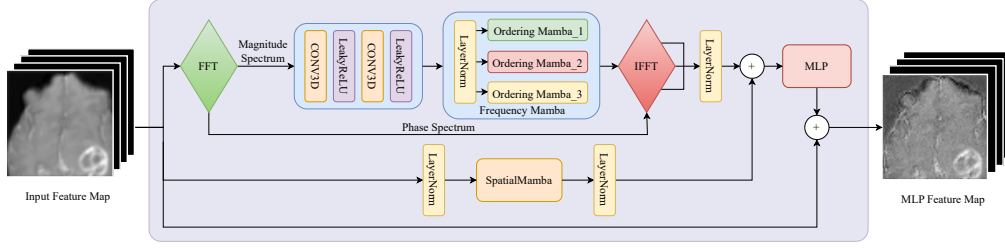


Figure 3: The detailed architecture of the proposed MDIF Block.

continuous systems and incorporating input-dependent parameters. It is specifically designed for long-sequence modeling, with its core mathematical formulation as follows:

$$\begin{aligned} h'(t) &= Ah(t) + Bx(t), \\ y(t) &= Ch(t) + Dx(t). \end{aligned} \quad (3)$$

Traditional SSMs rely on fixed matrices (A, B, C), limiting their capacity to capture context-sensitive dynamics. Mamba addresses this by introducing a selective mechanism, where B and C are dynamically generated via input-conditioned linear projections, enabling adaptive feature representation. Matrix A is initialized using the HiPPO framework to enhance long-term memory and efficient compression of historical information. This design allows the model to selectively emphasize salient elements—such as key linguistic units in NLP—while suppressing irrelevant content.

Given Mamba’s sensitivity to input sequence order and its limited capacity for local spatial modeling, we leverage the structural properties of frequency domain information—symmetry and directional distribution—to design a multi-directional scanning mechanism tailored for 3D frequency domain information. This strategy effectively balances global context modeling with local feature extraction.

3.2 Architecture

The overall architecture of our model is illustrated in Fig.2. The proposed model architecture adopts an encoder-decoder framework, where the encoder incorporates a dual-branch Multi-domain Information Fusion Mamba module. This module employs a dual-branch design to extract features from images at multiple scales, enabling efficient cross-scale feature fusion that comprehensively captures both global and local contextual information. In the decoder, transposed convolutions are employed for upsampling, while skip connections and residual connections are integrated to enhance feature fusion. This feature fusion process is repeated hierarchically, and finally, the decoder progressively reconstructs the original image size to produce the final segmentation output. Subsequent sections elaborate on the design principles and implementation details of each sub-module.

Multi-domain Information Fusion Block As illustrated in Fig.3, the Multi-domain Information Fusion Mamba architecture comprises two primary branches designed to effectively integrate information from multiple domains, thereby enhancing model performance.

Frequency Domain Branch. For each frequency domain branch, the input feature $F_{i,j}$ is first transformed into fre-

quency domain information F_{fre} using the Fast Fourier Transform (FFT). Since frequency domain data are inherently complex numbers, they are decomposed into the magnitude spectrum F_{mag} and the phase spectrum F_{pha} . The normalized magnitude spectrum is then fed into a convolutional neural network (CNN) module to extract detailed features. These features, in conjunction with a 3D multi-directional scanning mechanism (which will be elaborated upon in the following section), are input into the Mamba module to capture global features:

$$\begin{aligned} F_{fre} &= FFT(F_{i,j}), \\ F_{mag} &= LayerNorm(ABS(F_{fre})), \\ F_{pha} &= ANGLE(F_{fre}), \\ F_m &= LR(ConvBlock_{1*1*1}(LR(ConvBlock_{1*1*1}(F_{mag})))), \\ F_1, F_2, F_3 &= MDSMBlock(F_m), \\ F_k &= Mamba(F_k), (k = 1, 2, 3), \\ F_{fre_k} &= IFFT(LayerNorm(F_k, F_{pha})), \end{aligned} \quad (4)$$

where FFT and IFFT denote the Fourier Transform and the Inverse Fourier Transform, respectively. In frequency domain image processing, the ABS and ANGLE operations are used to extract the magnitude and phase spectra from the complex representation of a frequency domain image, respectively. Correspondingly, these features are denoted as F_{mag} (magnitude feature) and F_{pha} (phase feature). LR denotes the LeakyReLU, and MDSMBlock denotes 3D Multi-Directional Scanning Mechanism Block, which divides frequency domain information sequences into three different directional sequences.

Spatial Domain Branch. For each spatial domain branch, input feature $F_{i,j}$ is normalized through layer normalization and then fed into the Mamba module to extract features. These features are subsequently unified in both dimensionality and channels with the frequency domain information.

$$F_{spa} = Mamba(LayerNorm(F_{i,j})). \quad (5)$$

Multi-domain Information Fusion. After both branches have extracted spatial and frequency domain features, respectively, the frequency domain image is converted back to the spatial domain using the inverse Fourier transform. The multi-directional frequency domain images are then aligned, and their features are fused and enhanced through element-wise addition. An MLP module is employed to achieve superior fusion performance.

$$\begin{aligned} F_{fus} &= MLP(F_{spa} + F_{fre1} + F_{fre2} + F_{fre3}), \\ F_{i,j,out} &= F_{i,j} + F_{fus}. \end{aligned} \quad (6)$$

The MLP module comprises twice $1 \times 1 \times 1$ 3D convolution followed by a GELU nonlinearity. Finally, a residual

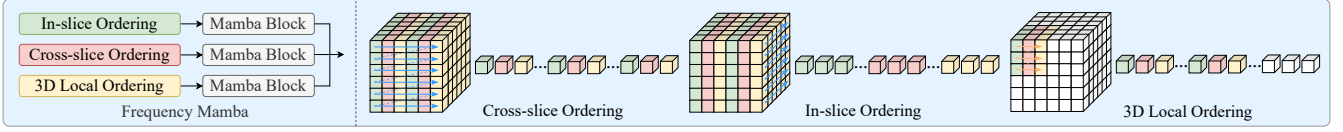


Figure 4: The detailed architecture of the proposed Frequency Mamba, a 3D multi-directional scanning mechanism.

connection adds the input features to the processed output, and the result is forwarded to the subsequent module.

3D Multi-Directional Scanning Mechanism The original Mamba sequence scanning is designed for modeling unidirectional sequences, making it less suitable for image processing, especially for high-dimensional 3D medical images. In 2D images, scanning mechanisms have been proposed, horizontally and vertically (both forward and reverse), among other directions (Huang et al. 2024). For 3D image scanning, a 2D scanning mechanism is applied to each individual slice, and the slices are then concatenated sequentially. Our scanning mechanism takes full advantage of the inherent properties of 3D images as well as the corresponding relationships in frequency domain features.

In image processing, spatial domain data exhibits prominent conjugate symmetry characteristics when transformed into the frequency domain via Fourier transform. Leveraging inherent symmetry, the transformed 1D sequence exhibits mirrored halves, preserving bidirectional representational capacity. Our proposed 3D multi-directional scanning mechanism enables simultaneous capture of both forward and reverse frequency spectrum information through forward scanning, the scanning mechanism is illustrated in Fig.4. This design not only achieves significant improvement in scanning efficiency, but also effectively integrates global contextual features with local detail information within a single scanning sequence. Specifically tailored for the properties of 3D medical imaging data and guided by the distinctive properties of frequency-domain information, we develop three specialized feature extraction pathways: in-slice ordering focuses on intra-slice feature modeling, cross-slice ordering specializes in inter-slice correlation analysis, and 3D local ordering enhances characterization of spatial volumetric relationships. This synergistic fusion of multi-dimensional features can significantly enhance global contextual awareness while maintaining local detail precision.

Decoder Block As illustrated in Fig.2, transposed convolutions are initially employed to upsample the spatial dimensions of the lower module’s feature maps. Subsequently, these upsampled feature maps are concatenated with the corresponding skip connection feature maps from the encoder, and two convolutional layers are utilized to achieve feature fusion and restore high-resolution representations. Additionally, residual connections are incorporated to facilitate effective deep-network training.

3.3 Loss Function

Our task is to classify every voxel in 3D medical images into one of four categories. Therefore, we use the CrossEn-

ropyLoss function, which is commonly employed in classification tasks to compute the cross-entropy between the predicted distribution and the target distribution. The loss is calculated as follows:

$$L = - \sum_{i=1}^N \log \left(\frac{e^{z_{y_i}}}{\sum_j e^{z_j}} \right), \quad (7)$$

where z represents the logits for each class, and z_{y_i} is the logit corresponding to the true class for voxel i .

4 Experiments

4.1 Datasets and implementation

Datasets. We evaluate our proposed approach with the BraTS2023 (Menze et al. 2014; Kazerooni et al. 2024) and BraTS2020 (Bakas et al. 2017, 2018) datasets, which comprise 1251 and 251 3D MRI scans of patients with diffuse gliomas, respectively. Each patient’s scan includes four modalities (T1, T1c, T2, and FLAIR) and three segmentation targets (WT:Whole Tumor, TC:Tumor Core, and ET:Enhancing Tumor).

Implementation details. Our model was implemented using Python 3.10.13 and PyTorch 2.1.1 with NVIDIA 3090 GPUs and CUDA version 11.8. All 3D medical images were randomly cropped to dimensions of $128 \times 128 \times 128$ for model training, with a batch size set to 2. We employed the SGD optimizer to update gradient information, setting the learning rate to $1e-2$ with a decay rate of $1e-5$. The datasets were divided into a training set (80%) and a test set (20%).

4.2 Comparison with State-of-the-art Methods

We compare our proposed SSFMamba with several state-of-the-art segmentation methods, including CNN-based approaches (U-Net (Ronneberger, Fischer, and Brox 2015), UX-Net (Ji et al. 2020), MedNeXt (Roy et al. 2023)), SuperLightNet (Yu et al. 2025), Transformer-based approaches (UNETR (Hatamizadeh et al. 2022), SwinUNETR (Cao et al. 2022), SwinUNETR-V2 (He et al. 2023), TransUNet (Chen et al. 2024)), and Mamba-based approaches (SegMamba (Xing et al. 2024), EM-Net (Chang et al. 2024)). To ensure a fair comparison, we retrained these models under the same settings and data processing procedures.

As presented in Tab.1, we can observe that the proposed approach achieves the best performance compared to other methods. Notably, in terms of HD95, the incorporation of frequency domain features enhances global contextual understanding, leading to superior boundary alignment. Moreover, on the BraTS2023 dataset—which features a larger and more diverse set of cases—our method consistently outperforms all competing approaches. Our approach demonstrates a statistically significant 0.83% improvement over

Methods	Architecture	WT		TC		ET		Avg	
		Dice↑	HD95↓	Dice↑	HD95↓	Dice↑	HD95↓	Dice↑	HD95↓
U-Net 2015	CNN	92.83	4.17	92.15	3.76	86.75	4.20	90.58	4.05
UXNET 2020		<u>94.55</u>	3.69	92.63	4.29	86.98	3.86	91.39	3.95
MedNext 2023		93.94	3.57	91.42	3.68	88.41	3.92	91.26	3.72
SuperLightNet 2025		94.42	3.94	<u>93.76</u>	3.28	88.61	3.74	92.26	3.65
UNETR 2022	Transformer	93.30	4.88	90.02	5.88	86.56	5.35	89.96	5.37
SwinUNETR 2022		93.77	4.10	90.14	4.45	87.07	4.38	90.33	4.31
SwinUNETR-V2 2023		93.57	4.03	92.89	4.38	88.97	3.92	91.81	4.11
TransUNet 2024		92.44	4.31	87.57	4.41	81.65	4.73	87.22	4.48
EM-Net 2024	Mamba	93.04	<u>3.53</u>	92.53	3.79	88.84	4.03	91.47	3.78
SegMamba 2024		93.57	3.69	93.55	<u>3.04</u>	<u>89.76</u>	3.31	<u>92.30</u>	<u>3.35</u>
SSFMamba (Ours)	Mamba	94.69	3.41	94.78	2.96	89.92	<u>3.43</u>	93.13	3.26

Table 1: Quantitative comparison on the BraTS2023 Dataset, the best two results are highlighted in bold and underline.

Methods	Architecture	WT		TC		ET		Avg	
		Dice↑	HD95↓	Dice↑	HD95↓	Dice↑	HD95↓	Dice↑	HD95↓
U-Net 2015	CNN	89.79	4.91	84.01	5.56	74.82	8.01	82.87	6.16
UXNET 2020		90.09	4.62	83.32	5.60	<u>76.19</u>	8.06	83.20	6.09
MedNext 2023		<u>91.26</u>	4.75	83.52	4.77	75.71	8.01	83.49	5.84
SuperLightNet 2025		90.68	7.89	83.16	5.65	76.31	7.71	83.38	6.88
UNETR 2022	Transformer	90.13	6.05	78.93	6.11	73.89	8.72	80.98	6.96
SwinUNETR 2022		90.10	5.13	84.11	5.54	75.52	7.91	83.24	6.19
SwinUNETR-V2 2023		90.37	5.16	83.83	5.40	75.18	<u>7.58</u>	83.13	6.04
TransUNet 2024		89.35	<u>4.34</u>	80.34	5.67	71.47	8.64	80.38	6.22
EM-Net 2024	Mamba	90.81	5.04	83.44	5.77	75.65	8.08	83.30	6.29
SegMamba 2024		90.77	4.38	<u>84.33</u>	6.17	75.98	8.04	<u>83.69</u>	6.20
SSFMamba (Ours)	Mamba	91.31	4.31	84.51	<u>4.97</u>	76.69	7.53	84.17	5.60

Table 2: Quantitative comparison on the BraTS2020 Dataset, the best two results are highlighted in bold and underline.

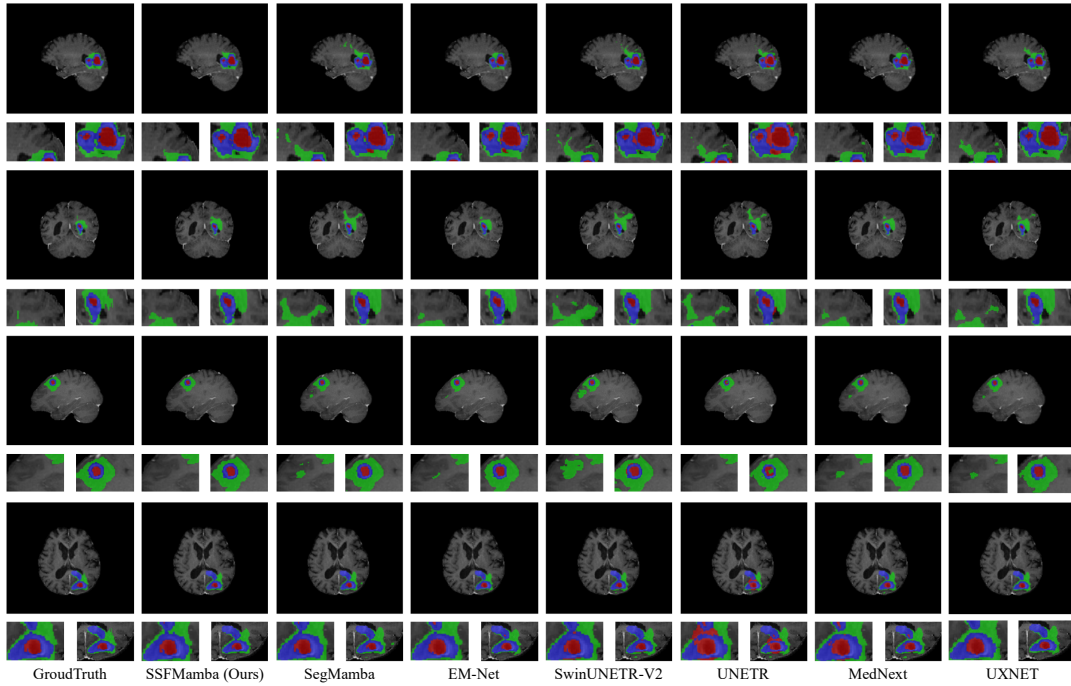


Figure 5: Qualitative comparison on the BraTS2023 Dataset. The annotated regions are categorized into three classes: red indicates NCR (necrotic tumor core), blue indicates ET (GD-enhancing tumor), and green indicates ED (the peritumoral edematous/invaded tissue). Below each image, a magnified view of the corresponding region is provided to highlight the differences in fine-grained segmentation performance across methods.

Methods	WT		TC		ET		Avg	
	Dice↑	HD95↓	Dice↑	HD95↓	Dice↑	HD95↓	Dice↑	HD95↓
baseline	93.33	3.91	92.77	3.40	88.09	3.87	91.40	3.77
baseline + FDB	93.68	3.40	92.79	<u>3.04</u>	90.96	3.66	<u>92.46</u>	<u>3.37</u>
baseline + MDSM	<u>94.31</u>	3.59	92.00	3.09	89.23	3.61	91.85	3.43
baseline + MDSM2	92.79	3.83	<u>92.92</u>	3.45	89.46	3.29	91.73	3.43
baseline → CNN	92.60	4.39	90.21	4.69	85.96	4.24	89.59	4.44
baseline → Transformer	93.23	4.02	92.41	3.55	87.73	3.96	91.12	3.84
SSFMamba	94.69	<u>3.41</u>	94.78	2.96	<u>89.92</u>	<u>3.43</u>	93.13	3.26

Table 3: Ablation study for the effectiveness of each component on the BraTS2023 Dataset.

Methods	WT		TC		ET		Avg	
	Dice↑	HD95↓	Dice↑	HD95↓	Dice↑	HD95↓	Dice↑	HD95↓
1 Layer	94.21	<u>3.59</u>	92.26	<u>3.14</u>	88.25	3.58	91.57	<u>3.44</u>
2 Layers (SSFMamba)	94.69	3.41	94.78	2.96	89.92	3.43	93.13	3.26
3 Layers	92.83	4.23	<u>93.53</u>	3.44	<u>89.72</u>	<u>3.57</u>	<u>92.03</u>	3.75

Table 4: Comparison of different network layers on the BraTS2023 Dataset.

the second-best method, demonstrating its robustness and effectiveness in handling complex segmentation tasks. To more intuitively validate the superior performance of our method, we further visualize the segmentation results of the various methods on the BraTS2023 dataset, as illustrated in Fig.5. We can observe that the compared methods are more likely to over-segment or under-segment, especially on subtle edges. In contrast, even in complex segmentation scenarios, our approach delineates the boundaries of various labels more clearly. Additionally, in terms of local details, our method achieves more refined segmentation.

4.3 Ablation Analysis

We conduct ablation studies on the BraTS2023 dataset to assess the contributions of various components within our overall model. As presented in Tab.3 and Tab.4, in our base model, we remove all additional modules and rely solely on a spatial domain model combined with the Mamba module for feature extraction. The results show a significant performance drop, primarily because the absence of frequency domain information weakens the model’s ability to capture global context. Our proposed 3D multi-directional scanning mechanism(MDSM) enhances the modeling of local relationships in the spatial domain. By comparing In-slice Ordering and Cross-slice Ordering(MDSM.2) with other experimental settings, we demonstrate the effectiveness of MDSM and the importance of 3D local ordering. However, due to the absence of the conjugate symmetry inherent in spatial domain data, its performance gains in this domain are limited. By leveraging the unique properties of frequency domain representations, this mechanism demonstrates superior modeling effectiveness when applied in the frequency domain. Furthermore, removing the 3D multi-directional scanning mechanism from the frequency domain Mamba and fusing its output with that of the spatial domain Mamba leads to some performance improvement. However, the segmentation of local details remains constrained and does not achieve the highest overall performance. In addition, we compared models based on CNN

and Transformer backbones, both of which underperformed compared to our Mamba-based design. This is because the multi-directional scanning mechanism is specifically tailored for the sequence-sensitive nature of Mamba, enhancing its local modeling capacity while preserving global feature extraction. Each MDIF Encoder module incorporates two MDIF blocks. For comparison, we also develop encoder configurations containing a single MDIF block and one with three MDIF blocks. Quantitative evaluations demonstrate that our design with two MDIF blocks delivers superior performance. These ablation experiments demonstrate the rationale and effectiveness of our designed modules.

Conclusion

In this paper, we propose SSFMamba, a Mamba-based, symmetry-driven spatial–frequency feature fusion network designed to achieve accurate 3D medical image segmentation. SSFMamba captures global contextual relationships from frequency domain representations and fuses heterogeneous features from both the spatial and frequency domains. The key distinction of our model lies in its novel use of the Mamba block to process data in the frequency domain, which fully leverages the intrinsic conjugate symmetry of frequency representation. The synergistic interaction between the Mamba architecture and spectrum information substantially enhances global modeling capability. Furthermore, by incorporating a 3D multi-directional scanning mechanism tailored to the structural properties of frequency domain data, our approach achieves an optimal balance between local detail preservation and global context understanding. Comprehensive experiments on two datasets from the Brain Tumor Segmentation Challenge demonstrate the effectiveness of SSFMamba. By robustly integrating global contextual cues with local structural features, our framework shows potential as a foundation for future research in 3D medical image segmentation.

References

- Bakas, S.; Akbari, H.; Sotiras, A.; Bilello, M.; Rozycki, M.; Kirby, J. S.; Freymann, J. B.; Farahani, K.; and Davatzikos, C. 2017. Advancing the cancer genome atlas glioma MRI collections with expert segmentation labels and radiomic features. *Scientific data*, 4(1): 1–13.
- Bakas, S.; Reyes, M.; Jakab, A.; Bauer, S.; Rempfler, M.; Crimi, A.; Shinohara, R. T.; Berger, C.; Ha, S. M.; Rozycki, M.; et al. 2018. Identifying the best machine learning algorithms for brain tumor segmentation, progression assessment, and overall survival prediction in the BRATS challenge. *arXiv preprint arXiv:1811.02629*.
- Cao, H.; Wang, Y.; Chen, J.; Jiang, D.; Zhang, X.; Tian, Q.; and Wang, M. 2022. Swin-unet: Unet-like pure transformer for medical image segmentation. In *ECCV'22*, 205–218.
- Chang, A.; Zeng, J.; Huang, R.; and Ni, D. 2024. EM-Net: Efficient Channel and Frequency Learning with Mamba for 3D Medical Image Segmentation. In *MICCAI'23*, 266–275.
- Chen, J.; Mei, J.; Li, X.; Lu, Y.; Yu, Q.; Wei, Q.; Luo, X.; Xie, Y.; Adeli, E.; Wang, Y.; et al. 2024. TransUNet: Rethinking the U-Net architecture design for medical image segmentation through the lens of transformers. *Medical Image Analysis*, 97: 103280.
- Chi, L.; Jiang, B.; and Mu, Y. 2020. Fast fourier convolution. *Advances in Neural Information Processing Systems*, 33: 4479–4488.
- Gu, A.; and Dao, T. 2024. Mamba: Linear-time sequence modeling with selective state spaces. In *COLM'24*.
- Gu, A.; Goel, K.; and Ré, C. 2022. Efficiently modeling long sequences with structured state spaces. In *ICLR'22*.
- Hatamizadeh, A.; Tang, Y.; Nath, V.; Yang, D.; Myronenko, A.; Landman, B.; Roth, H. R.; and Xu, D. 2022. Unetr: Transformers for 3d medical image segmentation. In *WACV'22*, 574–584.
- He, Y.; Nath, V.; Yang, D.; Tang, Y.; Myronenko, A.; and Xu, D. 2023. Swinunetr-v2: Stronger swin transformers with stagewise convolutions for 3d medical image segmentation. In *MICCAI'23*, 416–426.
- Huang, J.; Liu, Y.; Zhao, F.; Yan, K.; Zhang, J.; Huang, Y.; Zhou, M.; and Xiong, Z. 2022. Deep fourier-based exposure correction network with spatial-frequency interaction. In *ECCV'22*, 163–180.
- Huang, T.; Pei, X.; You, S.; Wang, F.; Qian, C.; and Xu, C. 2024. Localmamba: Visual state space model with windowed selective scan. In *ECCV'24*, 12–22.
- Ji, Y.; Zhang, R.; Li, Z.; Ren, J.; Zhang, S.; and Luo, P. 2020. Uxnet: Searching multi-level feature aggregation for 3d medical image segmentation. In *MICCAI'20*, 346–356.
- Kazerooni, A. F.; Khalili, N.; Liu, X.; Haldar, D.; Jiang, Z.; Anwar, S. M.; Albrecht, J.; Adewole, M.; Anazodo, U.; Anderson, H.; et al. 2024. The brain tumor segmentation (BraTS) challenge 2023: focus on pediatrics (CBTN-CONNECT-DIPGR-ASNR-MICCAI BraTS-PEDs). *ArXiv*, arXiv–2305.
- LeCun, Y.; Bengio, Y.; et al. 1995. Convolutional networks for images, speech, and time series. *The Handbook of Brain Theory and Neural Networks*, 3361(10): 1995.
- Liu, J.; Yang, H.; Zhou, H.-Y.; Xi, Y.; Yu, L.; Li, C.; Liang, Y.; Shi, G.; Yu, Y.; Zhang, S.; et al. 2024a. Swin-umamba: Mamba-based unet with imagenet-based pretraining. In *MICCAI'24*, 615–625.
- Liu, S.; Yin, S.; Qu, L.; and Wang, M. 2023. Reducing Domain Gap in Frequency and Spatial Domain for Cross-Modality Domain Adaptation on Medical Image Segmentation. In *AAAI'23*, 1719–1727.
- Liu, X.; Zhang, C.; and Zhang, L. 2024. Vision mamba: A comprehensive survey and taxonomy. *arXiv preprint arXiv:2405.04404*.
- Liu, Y.; Tian, Y.; Zhao, Y.; Yu, H.; Xie, L.; Wang, Y.; Ye, Q.; Jiao, J.; and Liu, Y. 2024b. Vmamba: Visual state space model. *Advances in Neural Information Processing Systems*, 37: 103031–103063.
- Liu, Z.; Lin, Y.; Cao, Y.; Hu, H.; Wei, Y.; Zhang, Z.; Lin, S.; and Guo, B. 2021. Swin transformer: Hierarchical vision transformer using shifted windows. In *ICCV'21*, 10012–10022.
- Menze, B. H.; Jakab, A.; Bauer, S.; Kalpathy-Cramer, J.; Farahani, K.; Kirby, J.; Burren, Y.; Porz, N.; Slotboom, J.; Wiest, R.; et al. 2014. The multimodal brain tumor image segmentation benchmark (BRATS). *IEEE Transactions on Medical Imaging*, 34(10): 1993–2024.
- Plewes, D. B.; and Kucharczyk, W. 2012. Physics of MRI: a primer. *Journal of Magnetic Resonance Imaging*, 35(5): 1038–1054.
- Pratt, H.; Williams, B.; Coenen, F.; and Zheng, Y. 2017. Fcnn: Fourier convolutional neural networks. In *ECML PKDD'17*, 786–798.
- Rhee, H.; Jang, Y. I.; Kim, S.; and Cho, N. I. 2022. LC-FDNet: Learned lossless image compression with frequency decomposition network. In *CVPR'22*, 6033–6042.
- Ronneberger, O.; Fischer, P.; and Brox, T. 2015. U-net: Convolutional networks for biomedical image segmentation. In *MICCAI'15*, 234–241.
- Roy, S.; Koehler, G.; Ulrich, C.; Baumgartner, M.; Petersen, J.; Isensee, F.; Jaeger, P. F.; and Maier-Hein, K. H. 2023. Mednext: transformer-driven scaling of convnets for medical image segmentation. In *MICCAI'23*, 405–415.
- Smith, J. T.; Warrington, A.; and Linderman, S. W. 2023. Simplified state space layers for sequence modeling. In *ICLR'23*.
- Vaswani, A.; Shazeer, N.; Parmar, N.; Uszkoreit, J.; Jones, L.; Gomez, A. N.; Kaiser, Ł.; and Polosukhin, I. 2017. Attention is all you need. *Advances in Neural Information Processing Systems*, 30.
- Velisavljevic, V.; Beferull-Lozano, B.; and Vetterli, M. 2007. Space-frequency quantization for image compression with directionlets. *IEEE Transactions on Image Processing*, 16(7): 1761–1773.
- Walker, J. S. 2017. *Fast fourier transforms*. CRC press.

Wang, W.; Wang, J.; Chen, C.; Jiao, J.; Sun, L.; Cai, Y.; Song, S.; and Li, J. 2023. Fremae: Fourier transform meets masked autoencoders for medical image segmentation. *arXiv preprint arXiv:2304.10864*.

Wenxuan, W.; Chen, C.; Meng, D.; Hong, Y.; Sen, Z.; and Jiangyun, L. 2021. Transbts: Multimodal brain tumor segmentation using transformer. In *MICCAI'21*, 109–119.

Xing, Z.; Ye, T.; Yang, Y.; Liu, G.; and Zhu, L. 2024. Segmamba: Long-range sequential modeling mamba for 3d medical image segmentation. In *MICCAI'24*, 578–588.

Xu, K.; Qin, M.; Sun, F.; Wang, Y.; Chen, Y.-K.; and Ren, F. 2020. Learning in the frequency domain. In *CVPR'20*, 1740–1749.

Yang, Y.; Yuan, G.; and Li, J. 2024. Sffnet: A wavelet-based spatial and frequency domain fusion network for remote sensing segmentation. *IEEE Transactions on Geoscience and Remote Sensing*.

Yu, F.; Cao, J.; Liu, L.; and Jiang, M. 2025. SuperLightNet: Lightweight Parameter Aggregation Network for Multimodal Brain Tumor Segmentation. In *CVPR'25*, 5197–5206.

Yue, Y.; and Li, Z. 2024. Medmamba: Vision mamba for medical image classification. *arXiv preprint arXiv:2403.03849*.

Zhao, Z.; Bai, H.; Zhang, J.; Zhang, Y.; Xu, S.; Lin, Z.; Timofte, R.; and Van Gool, L. 2023. Cddfuse: Correlation-driven dual-branch feature decomposition for multi-modality image fusion. In *CVPR'23*, 5906–5916.

Zhou, M.; Huang, J.; Li, C.; Yu, H.; Yan, K.; Zheng, N.; and Zhao, F. 2022. Adaptively learning low-high frequency information integration for pan-sharpening. In *ACM MM'22*, 3375–3384.

Zhu, L.; Liao, B.; Zhang, Q.; Wang, X.; Liu, W.; and Wang, X. 2024. Vision mamba: efficient visual representation learning with bidirectional state space model. In *ICML'24*, 62429–62442.

Zou, W.; Gao, H.; Yang, W.; and Liu, T. 2024a. Wave-mamba: Wavelet state space model for ultra-high-definition low-light image enhancement. In *ACM MM'24*, 1534–1543.

Zou, Z.; Yu, H.; Huang, J.; and Zhao, F. 2024b. Freqmamba: Viewing mamba from a frequency perspective for image de-raining. In *ACM MM'24*, 1905–1914.